

Limit cycles in quantum theories

Stanisław D. Głazek ¹

Institute of Theoretical Physics, Warsaw University
ul. Hoża 69, 00-681 Warsaw

and

Kenneth G. Wilson

Department of Physics, The Ohio State University
174 West 18th Ave., Columbus, Ohio 43210-1106

Abstract

Renormalization group limit cycles may be a commonplace for quantum Hamiltonians requiring renormalization, in contrast to experience to date with classical models of critical points, where fixed points are far more common. We discuss the simplest model Hamiltonian identified to date that exhibits a renormalization group limit cycle. The model is a discrete Hamiltonian with two coupling constants and a non-perturbative renormalization group that involves changes in only one of these couplings and is soluble analytically. The Hamiltonian is the discrete analog to a continuum Hamiltonian previously proposed by us.

1 Introduction

In 1971, one of us suggested that renormalization group equations could have limit cycle solutions as well as fixed points when the renormalization group equations involve two or more coupling constants [1]. The 1971 paper did not mention the possibility that renormalization group equations might have limit cycle solutions even for differential equations for only one coupling constant. But in 1993, the two of us defined a simple Hamiltonian that requires the renormalization of just a single bare coupling constant g_Λ , where Λ is the cutoff [2]. The bare coupling constant, we demonstrated, exhibits limit

¹Work supported in part by KBN Grant No. 2 P03B 016 18.

cycle behavior in the limit $\Lambda \rightarrow \infty$. To be precise the coupling constant g_Λ was found to decrease steadily as Λ increased, until g_Λ reached $-\infty$, after which it jumped to $+\infty$ and started its next cycle of steady decrease. However, we did not recognize or comment that this behavior constituted a limit cycle. Moreover, the Hamiltonian we defined is singular, in such a way that it presumably does not have well-defined s-wave scattering phase shifts. The model has well-defined bound states, and our renormalization group analysis was based on keeping the finite bound state energies fixed as $\Lambda \rightarrow \infty$.

The model Hamiltonian we published in 1993 has no known physical application. But in 1999, Bedaque, Hammer, and Van Kolck showed that a three-body Hamiltonian with two- and three-body delta function potentials and a cutoff in momentum space is renormalizable and that the three-body coupling approaches a limit cycle as the cutoff λ approaches ∞ [3], much as it does in our 1993 model. Bedaque et al built on earlier work of Thomas [4] and Efimov [5], that was recently reviewed by Nielsen, Fedorov, Jensen, and Garrido [6]. However, the mathematics of the three body system is complex, and it is surely useful to have simpler models to study that exhibit limit cycles too.

In this paper, we discuss a discretized version of the Hamiltonian we introduced in 1993. With a cutoff, the discretized model takes the form of a finite size matrix with discrete eigenvalues. The discrete matrix has a diagonal sub-matrix, plus two off-diagonal pieces with two coupling constants. The Hamiltonian requires renormalization in the limit of infinite cutoff. Just as in the continuum case, the renormalization can be constructed analytically and leads to a limit cycle in one of the two couplings, while the second coupling constant stays fixed. But the analytically obtained limit cycle is defined only for a discrete sequence of cutoffs, rather than for a continuously varying cutoff. Using numerical procedures, it is possible to define and compute a renormalization process with a continuously varying cutoff, but our studies with the continuous cutoff variation will not be discussed here.

The finite matrix Hamiltonians can be diagonalized numerically, when the cutoff is small enough. The renormalizability of the Hamiltonians we will discuss here can be demonstrated to high numerical accuracy with cutoffs small enough to allow numerical diagonalization. We will provide the demonstration with a comparison of the eigenvalues of two matrices with two different cutoffs, one of size 37x37, the other of size 42x42.

The Hamiltonian to be used in this paper has the form

$$H_{mn}(g_N, h_N) = (E_m E_n)^{1/2} [\delta_{mn} - g_N - i h_N s_{mn}] , \quad (1)$$

where m and n are integers. For $m = n$, $\delta_{mn} = 1$ and $s_{mn} = 0$. For $m \neq n$, $\delta_{mn} = 0$ and $s_{mn} = (m - n)/|m - n|$. The numbers $E_n = b^n$ with $b > 1$, are eigenvalues of the operator H_0 that has matrix elements $\langle m | H_0 | n \rangle = H_{mn}(0, 0)$. The eigenvalues are called kinetic energies of the corresponding eigenstates, $|n\rangle$. The remaining part of the Hamiltonian, $H_I = H - H_0$, is called an interaction, and $H_I(0, 0) = 0$. The largest energy allowed in the dynamics is $\Lambda_N = b^N$, which defines the ultraviolet cutoff so that the subscripts $m, n \leq N$.

The continuous version of this model [2] is recovered in the limit $b \rightarrow 1$. The discrete model itself has been discussed in the case $h_N = 0$ using similarity renormalization group idea [7] and Wegner's equation [8]. It was shown that the model exhibits asymptotic freedom for $h_N = 0$. Hamiltonians of Eq. (1) with $h_N = 0$ can be derived in a number of

ways, ranging from a discretization of a nonrelativistic Schrödinger equation for a particle on a plane with a two-dimensional δ -potential, to a discrete version of the transverse dynamics of partons in quantum field theory.

At first, the model with $h_N \neq 0$ does not appear much different from the one with $h_N = 0$. All Hamiltonians defined by Eq. (1) are hermitian and have a general ultraviolet logarithmically divergent structure. The divergence originates in the fact that the far off-energy-shell matrix elements of H_{mn} , i.e. those with $|m - n| \gg 1$, behave like $(E_m E_n)^{1/2}$. Therefore, perturbation theory produces large-energy contributions of the form $\sum_i (E_m E_i)^{1/2} (1/E_i) (E_i E_n)^{1/2}$, and every energy scale contributes a significant amount to the sum, which grows linearly with the number of initially included scales, $N = \ln \Lambda_N / \ln b$. The dependence of the unrenormalized coupling constants g_N and h_N on N , is expected to compensate this effect. As we will demonstrate below, when h_N is not zero, the model exhibits limit cycle behavior as N goes to infinity. We will prove this by deriving a renormalization group equation that determines g_{N-1} (used with a cutoff Λ_{N-1}), given g_N and h_N used with cutoff Λ_N , such that the low energy eigenvalues stay fixed.

This paper is organized as follows. Section 2 describes the discrete RG flow of the model Hamiltonians $H(g_N, h_N)$ with N . The structure of eigenstates of these Hamiltonians is also briefly described. Section 3 shows a numerical example of the spectrum of renormalized Hamiltonians and their discrete rescaling properties. The spectrum is found to contain a sequence of negative (bound state) eigenvalues, one per cycle. Section 4 concludes the paper.

2 Renormalization group trajectories

The eigenvalue problem

$$\sum_{n=-\infty}^N H_{mn} \psi_n = E \psi_m, \quad (2)$$

can be solved for ψ_m , $m \leq N$, assuming that one knows E , by using the Gaussian elimination procedure. In the first step one can express ψ_N in terms of all other components, ψ_n with $n < N$. In the next step, one expresses ψ_{N-1} in terms of components ψ_n with $n < N - 1$, and so on. In fact, this procedure can be carried out without knowing E if the eliminated energy scales are much larger than E . Thus, when one is interested in the eigenvalues of order b^M with $M \rightarrow -\infty$, one can eliminate states from some huge energy range between $\Lambda_N = b^N$ and some fixed $\Lambda_0 = b^{N_0}$, where N_0 is much smaller than N and still $\Lambda_0 \gg E$. The new, much smaller eigenvalue problem will have the cutoff Λ_0 and the corresponding coupling constants. When the recursion for the whole sequence of the coupling constants $(g_N, h_N), (g_{N-1}, h_{N-1}), \dots, (g_{N_0}, h_{N_0})$, is found, one can trace it back starting from some assumed finite values (g_0, h_0) at a finite N_0 and see what happens with (g_N, h_N) when the cutoff number $N \rightarrow \infty$.

To carry out the above procedure, it is convenient to introduce a small number $\tilde{E} = E/b^N$ and write the eigenstate components in the form $\psi_n = b^{n/2} \phi_n$ for all $n \leq N$. The eigenvalue Eq. (2) becomes:

$$\begin{aligned}
(1 - \tilde{E})\phi_N &= g_N\sigma_N + ih_N\sigma_{N-1} , \\
(1 - b\tilde{E})\phi_{N-1} &= g_N\sigma_N + ih_N(-\phi_N + \sigma_{N-2}) , \\
(1 - b^2\tilde{E})\phi_{N-2} &= g_N\sigma_N + ih_N(-\phi_N - \phi_{N-1} + \sigma_{N-3}) , \\
&\vdots \\
(1 - b^n\tilde{E})\phi_{N-n} &= g_N\sigma_N + ih_N(-\phi_N + \dots - \phi_{N-n+1} + \sigma_{N-n-1}) , \\
&\vdots
\end{aligned}$$

where $\sigma_i = \sum_{j=-\infty}^i \phi_j$. If E and n are finite and $N \rightarrow \infty$, $b^i \tilde{E}$ for $i = 0, 1, \dots, n$ on the left hand sides of the above equations do not count. The first step of the Gaussian procedure gives

$$\phi_N = (g_N + ih_N)\sigma_{N-1}/(1 - g_N) . \quad (3)$$

Substituting this result into the remaining equations, one obtains a new set that does not explicitly involve the component with largest kinetic energy but has a different coupling constant instead. Namely,

$$\begin{aligned}
(1 - b\tilde{E})\phi_{N-1} &= g_{N-1}\sigma_{N-1} + ih_{N-1}\sigma_{N-2} , \\
(1 - b^2\tilde{E})\phi_{N-2} &= g_{N-1}\sigma_{N-1} + ih_{N-1}(-\phi_{N-1} + \sigma_{N-3}) , \\
&\vdots \\
(1 - b^n\tilde{E})\phi_{N-n} &= g_{N-1}\sigma_{N-1} + ih_{N-1}(-\phi_{N-1} + \dots - \phi_{N-n+1} + \sigma_{N-n-1}) , \\
&\vdots
\end{aligned}$$

The new coupling constant $g_{N-1} = g_N + (g_N^2 + h_N^2)/(1 - g_N)$, while $h_{N-1} = h_N$ stays unchanged. Making p such steps, one transforms (g_N, h_N) into (g_{N-p}, h_{N-p}) , where $h_{N-p} = h_N$ and

$$g_{N-p} = h_N \tan \left[\arctan \left(\frac{g_N}{h_N} \right) + p \arctan(h_N) \right] . \quad (4)$$

It is visible that $g_{N-p} = g_N$ when $h_N = \tan(\pi/p)$. Equation (4) demonstrates that the coupling constant g_N completes a cycle when Λ_N is reduced to Λ_N/b^p , and the cycle repeats itself in the further reductions. Fig. 1 shows these cycles for $\Lambda_{16} = b^{16}$, $g = 0.060606$ [8], and $h_{16} = \tan(\pi/5)$. If g_{16} were zero, the cycle would be symmetric with respect to the axis $g_N = 0$. On the other hand, components of the eigenvectors of $H(g_N, h_N)$ satisfy the recursion

$$\psi_n = b^{1/2} \frac{1 - ih_N - E/b^{n+1}}{1 + ih_N - E/b^n} \psi_{n+1}, \quad (5)$$

for all N and $n \leq N$ independently of the value of g_N .

Note that for real Hamiltonian matrices, i.e. for $h_N \rightarrow 0$, Eq. (4) implies

$$g_N = \frac{g_0}{1 + g_0(N - N_0)} , \quad (6)$$

which means asymptotic freedom, or $g_\Lambda = g_0/[1 + g_0 \ln(\Lambda/\Lambda_0)/\ln b] \rightarrow 0$ when $\Lambda \rightarrow \infty$. This is a fixed point behavior. In contrast, for complex Hamiltonians, Eq. (4) is equivalent

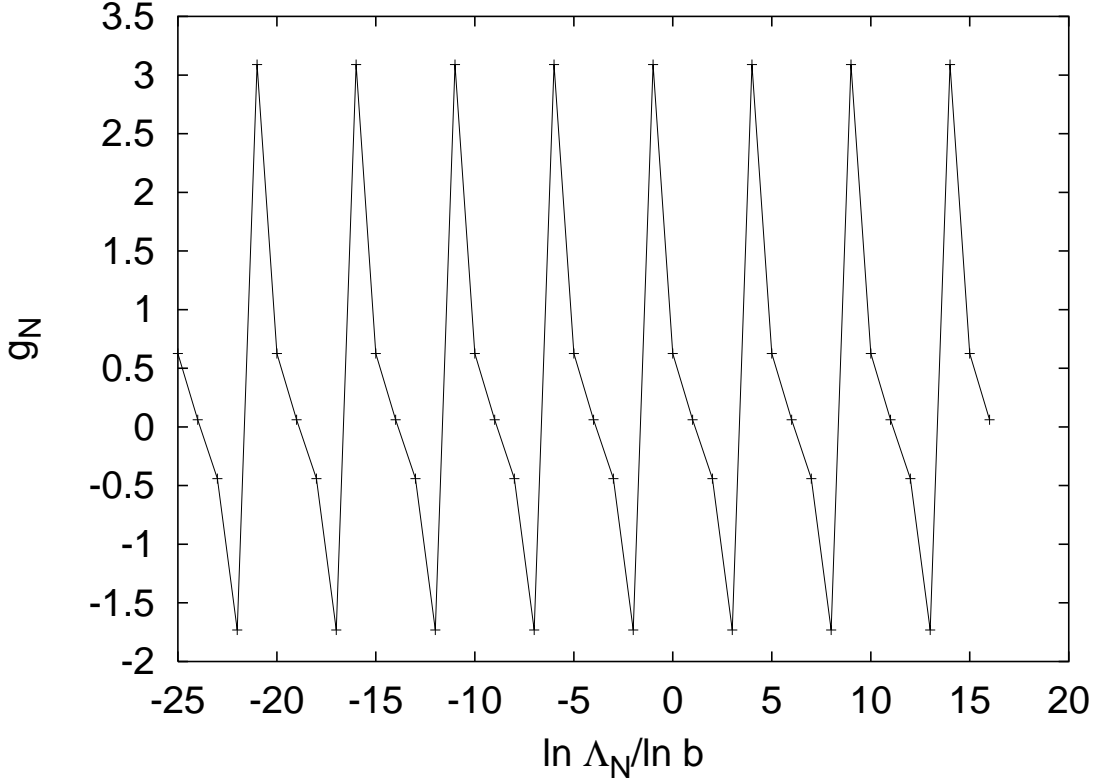


Figure 1: The discrete limit cycle dependence of the coupling constant g_N on the cutoff number $N = \ln \Lambda_N / \ln b$, $g_{16} = 0.060606$, $h_{16} = \tan(\pi/5)$. The lines are added between the discrete points only to guide the eye.

to the following renormalization group transformation of g_Λ from Λ_0 to Λ , ($h \equiv h_N = \text{const.}$),

$$g_\Lambda = h \frac{g_0 - h \tan [c \ln(\Lambda/\Lambda_0)]}{h + g_0 \tan [c \ln(\Lambda/\Lambda_0)]}, \quad (7)$$

where $c = \arctan(h)/\ln(b)$, which exhibits the limit cycle.

In the continuum limit of $b \rightarrow 1$, the sum over energy scales, $\sum_i \rightarrow \int d\Lambda/(\Lambda \ln b)$. When the ratio $r_c = \Lambda/\Lambda_0$ of two cutoffs separated by one complete cycle is kept constant and b tends to 1, the difference p between powers N and N_0 must grow to infinity, as $p = \ln r_c / \ln b$. The corresponding coupling constant $h = \tan(\pi/p)$ becomes then equal to $\pi/p = (\pi \ln b) / \ln r_c$ and the constant c in Eq. (7) becomes equal to $\pi / \ln r_c$. This result shows that the limit $b \rightarrow 1$ in the discrete model reproduces the continuum case from Ref. [2], and the period ratio is $r_c = \exp(\pi/c)$ for all values of the imaginary part c of the interaction term. The fixed-point behavior with asymptotic freedom is obtained only in the limit $c \rightarrow 0$, as the RG behavior in a one long cycle.

3 Numerical example

For illustration of the limit cycle from Fig. 1 and to show the existence of bound state solutions associated with it, Table 1 provides results of diagonalization of two Hamiltonian matrices: H_1 with m and n ranging from $M = -25$ to $N = 16$, and H_2 with $N = 11$ and the same M . Both Hamiltonians have the same values of $b = 2$, $h_{16} = h_{11} = \tan(\pi/5) \sim 0.726543$, and $g_{16} = g_{11} = 0.060606$ [8]. The Hamiltonian H_2 is considered a result of five discrete RG steps applied to the Hamiltonian H_1 . The infrared cutoff M was introduced in order to use a computer for calculations. The lower is M the better is the agreement between the example and the cycle theory applicable for $M \rightarrow -\infty$. The eigenvalues of small modulus (not too small, however, to stay away from the lower bound b^M) are identical in both cases within the displayed numerical accuracy. For these eigenvalues, the RG analysis of the previous section is fully confirmed. For eigenvalues close to the artificial lower bound b^M , the finite size of the matrix changes the pattern in a certain way, which is not relevant here.

The scaling phenomenon of interest is described by showing the ratios of ratios of successive eigenvalues for one matrix to two characteristic numbers. The negative eigenvalues, that correspond to bound states ($E_n = b^n$ are positive for all values of n), appear in a geometric sequence with quotient 32, with accuracy approaching several ppm in the best cases. Thus, there is one bound state per cycle among the solutions. The positive eigenvalues also appear in a geometric sequence, but with a quotient almost equal $2^{5/4}$, which can be understood on the basis of dimensional analysis without inspecting details of the solution. Namely, after p reduction steps one eliminates p states from the dynamics and obtains the Hamiltonian H_2 that is equivalent to $b^{-p}H_1 = H_1/32$. Since in every cycle among the p states only $p - 1$ have positive eigenvalues and the cycle repeats itself indefinitely, the ratio of the successive $p - 1$ eigenvalues (if such a common quotient exists) must satisfy the condition $r^{p-1} = b^p$ in order to scale properly from one cycle to another. Therefore, $r = b^{p/(p-1)}$, and in the example one obtains the factor $32^{1/4}$. Deviations from that rule within a single cycle cannot be understood so simply but the calculation shows a repeating sequence within a cycle with all elements very close to r .

However, the most prominent feature of the example is the appearance of one negative eigenvalue in every cycle. It requires further studies to be fully understood. Here it is noted that when the period p tends to infinity with $h_N \rightarrow 0$, one recovers the case from Ref. [8], with asymptotic freedom and a bound state, but in infinitely many copies connected together in a sequence. In every single long-cycle link in that chain, looked at in the direction of growing Λ , the asymptotically free coupling decreases logarithmically towards large energies until it eventually crosses zero, grows in size and turns up rapidly. A new generation bound state is uncovered at that scale, and a new cycle starts from a large coupling constant that decreases slowly again.

| n | $\Lambda = 2^{16}$ | r | $\Lambda = 2^{11}$ | r |
|-----|--------------------|----------|--------------------|----------|
| 13 | 0.954734+05 | - | - | - |
| 12 | 0.328953+05 | 0.819481 | - | - |
| 11 | 0.131845+05 | 0.953270 | - | - |
| 10 | 0.545303+04 | 0.983701 | - | - |
| 9 | 0.228087+04 | 0.994830 | 0.298354+04 | - |
| 8 | 0.956198+03 | 0.997093 | 0.102798+04 | 0.819481 |
| 7 | 0.401063+03 | 0.997590 | 0.412015+03 | 0.953270 |
| 6 | 0.168593+03 | 0.999803 | 0.170407+03 | 0.983701 |
| 5 | 0.709615+02 | 1.001090 | 0.712770+02 | 0.994830 |
| 4 | 0.298253+02 | 0.999652 | 0.298812+02 | 0.997093 |
| 3 | 0.125234+02 | 0.998679 | 0.125332+02 | 0.997590 |
| 2 | 0.526682+01 | 1.000260 | 0.526853+01 | 0.999803 |
| 1 | 0.221724+01 | 1.001270 | 0.221755+01 | 1.001090 |
| 0 | 0.931986+00 | 0.999731 | 0.932040+00 | 0.999652 |
| -1 | 0.391347+00 | 0.998713 | 0.391357+00 | 0.998679 |
| -2 | 0.164586+00 | 1.000270 | 0.164588+00 | 1.000260 |
| -3 | 0.692886-01 | 1.001280 | 0.692889-01 | 1.001270 |
| -4 | 0.291245-01 | 0.999733 | 0.291245-01 | 0.999731 |
| -5 | 0.122296-01 | 0.998714 | 0.122296-01 | 0.998713 |
| -6 | 0.514332-02 | 1.000270 | 0.514332-02 | 1.000270 |
| -7 | 0.216526-02 | 1.001280 | 0.216526-02 | 1.001280 |
| -8 | 0.910135-03 | 0.999730 | 0.910135-03 | 0.999730 |
| -9 | 0.382169-03 | 0.998705 | 0.382169-03 | 0.998705 |
| -10 | 0.160723-03 | 1.000250 | 0.160723-03 | 1.000250 |
| -11 | 0.676587-04 | 1.001230 | 0.676587-04 | 1.001230 |
| -12 | 0.284359-04 | 0.999610 | 0.284359-04 | 0.999610 |
| -13 | 0.119370-04 | 0.998423 | 0.119370-04 | 0.998423 |
| -14 | 0.501683-05 | 0.999594 | 0.501683-05 | 0.999594 |
| -15 | 0.210854-05 | 0.999630 | 0.210854-05 | 0.999630 |
| -16 | 0.882705-06 | 0.995684 | 0.882705-06 | 0.995684 |
| -17 | 0.367003-06 | 0.988875 | 0.367003-06 | 0.988875 |
| -18 | 0.150481-06 | 0.975210 | 0.150481-06 | 0.975210 |
| -19 | 0.584264-07 | 0.923457 | 0.584264-07 | 0.923457 |
| -22 | 0.654169-08 | 0.266298 | 0.654169-08 | 0.266298 |
| -4 | -.622117-06 | 0.964026 | -.622117-06 | 0.964026 |
| -3 | -.206506-04 | 0.998881 | -.206506-04 | 0.998880 |
| -2 | -.661561-03 | 0.999965 | -.661561-03 | 0.999960 |
| -1 | -.211707-01 | 0.999994 | -.211708-01 | 0.999831 |
| 0 | -.677466-00 | 0.999832 | -.677580+00 | 0.994617 |
| 1 | -.216826+02 | 0.994617 | -.217999+02 | 0.824124 |
| 2 | -.697598+03 | 0.824124 | -.846472+03 | - |
| 3 | -.270871+05 | - | - | - |

Table 1. The columns contain: n - the approximate integer powers of $2^{5/4}$ (2^5) that give positive (negative) eigenvalues; $\Lambda = 2^{16}$ - the eigenvalues of the Hamiltonian with $N = 16$ and $M = -25$ (see the text for details); r - the ratio of the ratio of two successive eigenvalues to $2^{5/4}$ (2^5) for the positive (negative) eigenvalues; $\Lambda = 2^{11}$ - the eigenvalues of H after 5 discrete RG steps (the same M is used).

4 Conclusion

The possibility of a long asymptotically free cycle due to small imaginary couplings, with an abrupt end and a bound state formation where a new cycle starts, is an interesting feature of our specific model. But the central result of our paper is that such a simple Hamiltonian exhibits limit cycle behavior for non-zero h instead of a fixed point. Together with the limit cycle found by Bedaque et al, and implicit in earlier work of Efimov and Thomas, this raises the question of whether limit cycle behavior is a common feature of renormalized quantum theories, outside of those that have already been solved and are known to exhibit fixed points. The model analysis carried out here certainly needs improvements, especially concerning details of the bound state formation and the sharp turn of the coupling where it approaches 1 and Eq. (4) produces a jump.

Separately from the existence of the limit cycle, the model is also valuable because it can be studied using the similarity RG technique (see [8]), and the latter can be applied to Hamiltonians in quantum field theories of major interest, such as QCD (see e.g. [9, 10]). (We do not expect QCD in particular to show limit cycle behavior: our comments about limit cycles apply more to broad classes of Hamiltonians, most not yet examined, rather than specific ones already examined as extensively as QCD has been.) The authors have generated numerical solutions to Wegner's differential equation in the model and found continuous similarity RG evolution of effective couplings with all key features described here. Thus, when one uses the similarity scheme in studies of effective Hamiltonians in more advanced models, one may also encounter complex RG scenarios. It remains to be seen if the model structure reappears in realistic quantum theories.

References

- [1] K. G. Wilson, Phys. Rev. D**3**, 1818 (1971).
- [2] St. D. Głazek and K. G. Wilson, Phys. Rev. D**47**, 4657 (1993).
- [3] P. F. Bedaque, H.-W. Hammer, U. van Kolck, Phys. Rev. Lett. **82**, 463 (1999).
- [4] L. H. Thomas, Phys. Rev. **47**, 903 (1935).
- [5] V. M. Efimov, Phys. Lett. **B33**, 563 (1970).
- [6] E. Nielsen, D. V. Fedorov, A. S. Jensen, E. Garrido, Phys. Rep. **347**, 373 (2001).
- [7] St. D. Głazek and K. G. Wilson, Phys. Rev. D**48**, 5863 (1993); *ibid.* D**49**, 4214 (1994).
- [8] St. D. Głazek and K. G. Wilson, Phys. Rev. D**57**, 3558 (1998); cf. F. Wegner, Ann. Physik **3**, 77 (1994).
- [9] K. G. Wilson et al., Phys. Rev. D**49**, 6720 (1994).
- [10] St. D. Głazek, Phys. Rev. D **63**, 116006 (2001).